The Astrophysical Journal, 929:41 (15pp), 2022 April 10 https://doi.org/10.3847/1538-4357/ac5745

Massive Molecular Gas Reservoir in a Luminous Submillimeter Galaxy during Cosmic Noon

Bin Liu[1,2], N. Chartab[2], H. Nayyeri[2], A. Cooray[2], C. Yang[3,4], D. A Riechers[5], M. Gurwell[6], Zong-hong Zhu[1,7], S. Serjeant[8], E. Borsato[9], M. Negrello[10], L. Marchetti[11,12,8], E. M. Corsini[9,13], and P. van der Werf[14]
[1] Department of Astronomy, Beijing Normal University, Beijing 100875, People's Republic of China; acooray@uci.edu
[2] Department of Physics and Astronomy, University of California, Irvine, CA92697, USA
[3] Joint ALMA Observatory, Alonso de Córdova 3107, Vitacura 763-0355, Santiago, Chile
[4] European Southern Observatory, Alonso de Córdova 3107, Vitacura, Casilla 19001, Santiago de Chile, Chile
[5] Cornell University, Space Sciences Building, Ithaca, NY 14853, USA
[6] Center for Astrophysics | Harvard & Smithsonian, 60 Garden Street, Cambridge, MA 02138, USA
[7] School of Physics and Technology, Wuhan University, Wuhan 430072, People's Republic of China
[8] School of Physical Sciences, The Open University, Milton Keynes, MK7 6AA, UK
[9] Dipartimento di Fisica e Astronomia "G. Galilei", Universit'di Padova, Vicolo dell'Osservatorio 3, I-35122, Padova, Italy
[10] School of Physics and Astronomy, Cardiff University, The Parade, Cardiff, CF24 3AA, UK
[11] Department of Astronomy, University of Cape Town, Private Bag X3, Ronderbosch, 7701 Cape Town, South Africa
[12] INAF—Istituto di Radioastronomia, via Gobetti 101, I-40129 Bologna, Italy
[13] INAF—Osservatorio Astronomico di Padova, vicolo dell'Osservatorio 5, I-35122 Padova, Italy
[14] Leiden University, Leiden Observatory, PO Box 9513, NL-2300 RA, Leiden, The Netherlands
Received 2021 August 29; revised 2022 February 9; accepted 2022 February 13; published 2022 April 11

Abstract

We present multiband observations of an extremely dusty star-forming lensed galaxy (HERS1) at $z = 2.553$. High-resolution maps of HST/WFC3, SMA, and ALMA show a partial Einstein ring with a radius of $\sim 3''$. The deeper HST observations also show the presence of a lensing arc feature associated with a second lens source, identified to be at the same redshift as the bright arc based on a detection of the [N II] 205 μm emission line with ALMA. A detailed model of the lensing system is constructed using the high-resolution HST/WFC3 image, which allows us to study the source-plane properties and connect rest-frame optical emission with properties of the galaxy as seen in submillimeter and millimeter wavelengths. Corrected for lensing magnification, the spectral energy distribution fitting results yield an intrinsic star formation rate of about $1000 \pm 260\,M_{\odot}$ yr^{-1}, a stellar mass $M_{*} = 4.3^{+2.2}_{-1.0} \times 10^{11} M_{\odot}$, and a dust temperature $T_{\rm d} = 35^{+2}_{-1}$ K. The intrinsic CO emission line ($J_{\rm up} = 3$, 4, 5, 6, 7, 9) flux densities and CO spectral line energy distribution are derived based on the velocity-dependent magnification factors. We apply a radiative transfer model using the large velocity gradient method with two excitation components to study the gas properties. The low-excitation component has a gas density $n_{\rm H_2} = 10^{3.8 \pm 0.6}$ cm^{-3} and kinetic temperature $T_{\rm k} = 18^{+7}_{-5}$ K, and the high-excitation component has $n_{\rm H_2} = 10^{3.1 \pm 0.4}$ cm^{-3} and $T_{\rm k} = 480^{+260}_{-220}$ K. Additionally, HERS1 has a gas fraction of about 0.19 ± 0.14 and is expected to last 100 Myr. These properties offer a detailed view of a typical submillimeter galaxy during the peak epoch of star formation activity.

Unified Astronomy Thesaurus concepts: Gravitational lensing (670); Submillimeter astronomy (1647); Galaxy formation (595)

Supporting material: animation

1. Introduction

The cold molecular gas (traced by millimeter observations of the molecular CO) is the key fuel for active star formation in galaxies (Carilli & Walter 2013). The fraction of the molecular gas reservoir that ends up in new stars (what is usually referred to as the star formation efficiency) depends on parameters such as the fragmentation and chemical compositions of the gas and is diminished by phenomena that disperse the gas and prevent the collapse, such as feedback from an active nucleus (AGN) or star-formation-driven winds (Bigiel et al. 2008; Sturm et al. 2011; Swinbank et al. 2011; Fu et al. 2012). Existing evidence suggests AGN activity is the dominant mechanism in quenching star formation at high redshifts, specifically in the most extreme environments (Cicone et al. 2014). On the other hand, the UV emission from newly born hot stars in star-forming regions ionizes the surrounding gas, generating a wealth of recombination nebular emission lines. The presence and intensity of these lines reveal valuable information on the physics of ionized gas surrounding these regions (Coil et al. 2015; Kriek et al. 2015; Shapley et al. 2015).

The most intense sites of star formation activities in the universe at high redshift happen in the gas-rich dusty star-forming galaxies (Casey et al. 2014). These heavily dust-obscured systems are often discovered in millimeter wavelengths and are believed to be the progenitors of the most massive red galaxies found at lower redshifts (Toft et al. 2014). Despite many efforts, the physics of the ionized gas (chemical composition, spatial extent, and relative line abundance) is still poorly understood for these star-forming factories of the universe. Recent resolved studies of ionized gas at high redshift mostly focus on normal star-forming galaxies and miss this hidden population of starbursting systems (Genzel et al. 2011; Förster Schreiber et al. 2014).

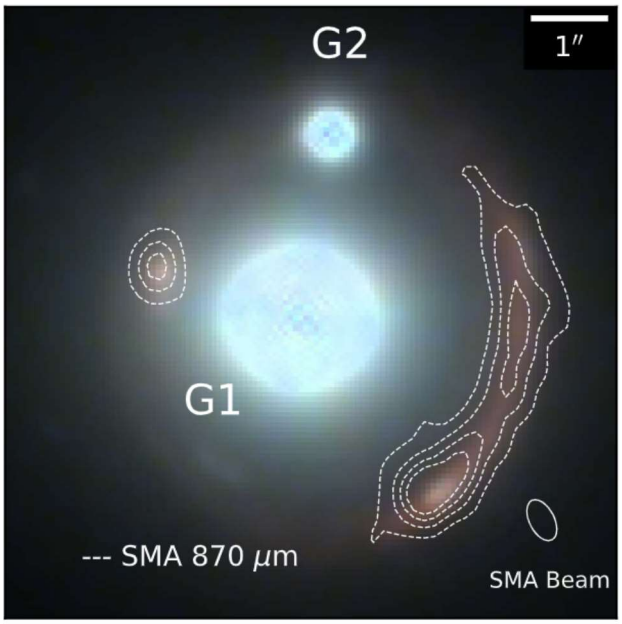

Figure 1. Three-color image of HERS1 adopting HST/WFC3 F110W (blue), F125W (green), and F160W (red) with submillimeter array (SMA) 870 μm contours overlaid. The SMA contours start from 9σ and increase in steps of 9σ with $\sigma = 305$ μJy beam^{-1}. The beam size is shown in the bottom right. Two deflecting galaxies at $z = 0.202$ (Geach et al. 2015) are marked as G1 and G2.

Submillimeter galaxies (SMGs) are more efficient in turning gas into stars than normal star-forming galaxies at the same epoch (i.e., Lyman-break galaxies (LBGs) and *BzK*-selected galaxies), similar to local ultraluminous infrared galaxies (ULIRGs) (Papadopoulos et al. 2012). Recent studies suggest that the LBG-selected star-forming galaxies might be fundamentally different from SMGs; whereas the former is usually characterized by SFR $< 100\,M_{\odot}$ yr^{-1}, the latter dominates the high-SFR end, and these are believed to be driven by different star formation mechanisms (Casey 2016). Using unlensed SMGs, Menéndez-Delmestre et al. (2013) showed that the star formation scale in these high-redshift systems seems to be very different from that of local starburst and are more extended over 2–3 kpc scales.

Through Herschel wide-area surveys, we have now identified hundreds of extremely bright submillimeter sources ($S_{500\mu m} \geqslant 100$ mJy) at high redshifts. After removing nearby contaminants, such bright 500 μm sources are either gravitationally lensed SMGs or multiple SMGs blended within the 18″ Herschel point spread function (PSF; Negrello et al. 2007, 2010, 2017), with most turning out to be strongly lensed SMGs in our high-resolution follow-up observations (Fu et al. 2012; Bussmann et al. 2013; Wardlow et al. 2013; Timmons et al. 2015). For this study, we have selected a very bright Keck/NIRC2-observed Einstein-ring-lensed SMG at $z = 2.553$ (HERS J020941.1+001557 designated as HERS1 hereafter; Figure 1). This target is identified from the Herschel Stripe 82 survey (Viero et al. 2014) covering 81 deg^2 with the Herschel/SPIRE instrument at 250, 350, and 500 μm. HERS1 at $z = 2.553$ is the brightest galaxy in Herschel extra-galactic maps and it is an Einstein ring with a radius of $\sim$3″. HERS1 has also been selected by other wide-area surveys such as Planck and ACT and has extensive follow-up observations from CFHT and HST in the near-infrared along with ancillary observations by JVLA, SCUBA-2, and ALMA with a CO redshift from the Redshift Search Receiver of the Large Millimeter Telescope and independently from Hα using the IRCS on Subaru (Geach et al. 2015; Harrington et al. 2016; Su et al. 2017). Here we report new data from Keck/NIRC2 Laser Guide Star Adaptive Optics (LGS-AO) imaging in H and K_s bands, HST/WFC3 F125W, Submillimeter Array (SMA), and ALMA. The wealth of multiband data combined with high-resolution deep imaging provides a unique opportunity to study the physical properties of HERS1 as an extremely bright SMG during the peak epoch of star formation activity.

This paper is organized as follows: In Section 2 we present observations and data reduction as well as previous archival data. In Section 3, we describe the lens-modeling procedures and reconstructed source-plane images of the high-resolution observations. We then show the source properties including the CO spectral line energy distribution (SLED), delensed CO spectral lines, large velocity gradient (LVG) modeling, as well as infrared spectral energy distribution (SED) fitting in Section 4. Finally, we summarize our results in Section 5.

Throughout this paper, we assume a standard flat-ΛCDM cosmological model with $H_0 = 70$ km s^{-1} Mpc^{-1} and $\Omega_\Lambda = 0.7$. All magnitudes are in the AB system.

2. Data

2.1. Hubble Space Telescope WFC3 Imaging

HERS1 was observed on 2018 September 02 under GO program 15475 in Cycle 25 with two orbits (PI: Nayyeri). We used the WFC3 F125W filter with a total exposure time of 5524 s. The data were reduced by the HST pipeline, resulting in a scale of 0.″128 pixel^{-1}. The photometry was performed following the WFC3 handbook (Rajan 2011).

2.2. Keck Near-IR Imaging

The near-IR data of HERS1 was observed with the KECK/NIRC2 Adaptive Optics system on 2017 August 27 (PID: U146; PI: Cooray). The H- and K_s-band filters were used at 1.60 μm and 2.15 μm, respectively. The observations were done with a custom nine-point dithering pattern for sky subtraction with 120 s (H band) and 80 s (K_s band) exposures per frame. Each frame has a scale of 0.″04 pixel^{-1}, adopting the wide camera in imaging mode. The data were reduced by a custom IDL routine (Fu et al. 2012).

2.3. Submillimeter Array

Observations of HERS1 were obtained in three separate configurations of the SMA as described below. In each configuration, observations of HERS1 were obtained in tracks shared with a second target. Generally, seven of the eight SMA antennas participated in the observations, except in one case (see below). The SMA operates in double-sideband mode, with sideband separation handled through a standard phase-switching procedure within the correlator (Ho et al. 2004). During the period, the new SMA SWARM correlator was expanding, resulting in increasing continuum bandwidth with each observation. All observations were obtained with a mean frequency between 341 and 343 GHz (870 μm).

HERS1 was first observed in the SMA subcompact configuration (maximum baselines $\sim$45 m) on 2016 September 20 (PID: 2016A-S007; PI: Cooray). The weather was good and stable, with a mean $\tau_{225\,\mathrm{GHz}}$ ranging from 0.07 to 0.09